Formate rescues neural tube defects caused by mutations in *Slc25a32*

Jimi Kim[a,1], Yunping Lei[b,1,2], Jin Guo[c], Sung-Eun Kim[b], Bogdan J. Wlodarczyk[b,2], Robert M. Cabrera[b,2], Ying Linda Lin[b,2], Torbjorn K. Nilsson[d], Ting Zhang[c], Aiguo Ren[e], Linlin Wang[e], Zhengwei Yuan[f], Yu-Fang Zheng[g,h], Hong-Yan Wang[g,h,3], and Richard H. Finnell[b,i,2,3]

[a]Department of Nutritional Sciences, Dell Pediatric Research Institute, Dell Medical School, University of Texas at Austin, Austin, TX 78723; [b]Department of Pediatrics, Dell Pediatric Research Institute, Dell Medical School, University of Texas at Austin , Austin, TX 78723; [c]Beijing Municipal Key Laboratory of Child Development and Nutriomics, Capital Institute of Pediatrics, 100700 Beijing, China; [d]Department of Medical Biosciences, Clinical Chemistry, Umea University, SE-90185 Umea, Sweden; [e]Institute of Reproductive and Child Health, Peking University, 100191 Beijing, China; [f]Key Laboratory of Health Ministry for Congenital Malformation, Shengjing Hospital, China Medical University, 117004 Shenyang, China; [g]Obstetrics & Gynecology Hospital, State Key Laboratory of Genetic Engineering and School of Life Sciences of Fudan University, 20043 Shanghai, China; [h]Key Laboratory of Reproduction Regulation of National Population and Family Planning Commission, Institute of Reproduction & Development and Children's Hospital of Fudan University, 200011 Shanghai, China; and [i]Collaborative Innovation Center for Genetics & Development, School of Life Sciences, Fudan University, 200438 Shanghai, China

Edited by Patrick J. Stover, Cornell University, Ithaca, NY, and approved March 28, 2018 (received for review January 4, 2018)

Periconceptional folic acid (FA) supplementation significantly reduces the prevalence of neural tube defects (NTDs). Unfortunately, some NTDs are FA resistant, and as such, NTDs remain a global public health concern. Previous studies have identified SLC25A32 as a mitochondrial folate transporter (MFT), which is capable of transferring tetrahydrofolate (THF) from cellular cytoplasm to the mitochondria in vitro. Herein, we show that gene trap inactivation of *Slc25a32* (*Mft*) in mice induces NTDs that are folate (5-methyltetrahydrofolate, 5-mTHF) resistant yet are preventable by formate supplementation. *Slc25a32*$^{gt/gt}$ embryos die in utero with 100% penetrant cranial NTDs. 5-mTHF supplementation failed to promote normal neural tube closure (NTC) in mutant embryos, while formate supplementation enabled the majority (78%) of knockout embryos to complete NTC. A parallel genetic study in human subjects with NTDs identified biallelic loss of function *SLC25A32* variants in a cranial NTD case. These data demonstrate that the loss of functional *Slc25a32* results in cranial NTDs in mice and has also been observed in a human NTD patient.

neural tube defects | Slc25a32 | folate | formate

Neural tube defects (NTDs) are one of the most common structural congenital malformations in humans, resulting from the failed closure of the neural tube before the fourth week after conception. The prevalence of NTDs ranges from 6.9 (Western Pacific) to 21.9 (Eastern Mediterranean) per 10,000 live births worldwide (1). Neural tube closure (NTC) is the morphological process occurring in early embryogenesis that will ultimately create the adult central nervous system, including the brain and spinal cord. The initiation of NTC involves the elevation of neural folds from the neural plate, ultimately fusing at the dorsal midline along the rostral-caudal embryonic axis (2). Common NTDs are phenotypically classified into anencephaly, myelomeningocele (spina bifida), craniorachischisis, and encephalocele with respect to the anatomical location of the defect (3).

Decades of research have shown that maternal folate insufficiency, interacting with genetic variants and environmental factors, contributes to the multifactorial risk for NTDs. As folate is required for multiple cellular processes, including nucleotide synthesis, DNA repair, genomic stability, mitochondrial protein synthesis, and methylation reactions including histone methylation, it is clear why deficiencies of one carbon (1C) donor molecules could contribute to failed NTC (4). In fact, the prevalence of NTDs was shown to be significantly reduced by up to >80% due to the protective effect of maternal FA supplementation (5), resulting in the recommendation that pregnant women should consume at least 400 μg/d (6). However, there remain a significant number of infants continuing to be born with NTDs that appear to be folate-resistant (7).

In mice, folate 1C metabolism occurs in balance between the cytosol and mitochondria. Reduced THF plays an important role in folate 1C metabolism, as either a 1C donor or acceptor, or transporting 1C groups through reciprocal conversions (4). Folate 1C metabolism supports de novo synthesis of purine, thymidylate, and homocysteine remethylation to methionine, supporting DNA replication and RNA production (8), and in the epigenetic regulation of DNA methylation (9). THF-dependent mitochondrial folate 1C metabolism produces formate, which is transported from the mitochondria into the cytoplasm to provide 1C units necessary for proper nucleotide biosynthesis and methylation reactions (4). At least 75% of the 1C units in cytoplasmic folate 1C metabolism are derived from the mitochondria (10), suggesting that the mitochondrial folate transport system plays a

Significance

Periconceptional supplementation with folic acid (FA) has reduced the prevalence of neural tube defects (NTDs) in numerous global populations; however, more than 30% of NTDs remain FA resistant. Previous in vitro studies identified *Slc25a32*-encoding mitochondrial folate transporter that delivers tetrahydrofolate across the mitochondrial membrane. Herein, we provide the original description of transgenic *Slc25a32* gene trapped (Slc25a32$^{gt/gt}$) knockout mice, who present with 100% penetrant NTDs. We demonstrate that formate supplementation rescues normal neural tube closure in the majority (78%) of *Slc25a32*$^{gt/gt}$ embryos, whereas 5-methyltetrahydrofolate was not effective. Additionally, biallelic *SLC25A32* loss-of-function mutations were identified in a human NTD case. Our findings add an NTD mouse model to several others that benefit developmentally from maternal formate supplementation.

Author contributions: J.K., Y.L., and R.H.F. designed research; J.K., Y.L., J.G., S.-E.K., B.J.W., R.M.C., Y.L.L., L.W., H.-Y.W., and R.H.F. performed research; J.K., Y.L., J.G., S.-E.K., B.J.W., R.M.C., T.K.N., T.Z., A.R., L.W., Z.Y., Y.-F.Z., H.-Y.W., and R.H.F. analyzed data; and J.K., Y.L., S.-E.K., B.J.W., R.M.C., T.Z., A.R., L.W., Z.Y., Y.-F.Z., H.-Y.W., and R.H.F. wrote the paper.

The authors declare no conflict of interest.

This article is a PNAS Direct Submission.

[1]J.K. and Y.L. contributed equally to this work.

[2]Present address: Departments of Molecular and Cellular Biology and Medicine, Baylor College of Medicine, Houston, TX 77030.

[3]To whom correspondence may be addressed. Email: wanghy@fudan.edu.cn or finnell@bcm.edu.

This article contains supporting information online at www.pnas.org/lookup/suppl/doi:10.1073/pnas.1800138115/-/DCSupplemental.

Published online April 16, 2018.

critical role in the folate 1C metabolism by transporting THF, a carrier of 1C units, in both the cytosol and the mitochondria.

The mitochondria folate transporter (MFT, encoded by *SLC25A32* gene) was initially described by the Moran laboratory and shown to be a basis for glycine auxotrophy (11–13). MFT is localized in the mitochondrial inner membrane (13) and transports THF from the cytosol to the mitochondria (4, 14). As far as we know, there are no functional studies of the *Slc25a32* gene during embryonic development, or on the influence of MFT on neural tube development and closure.

In this study, we created a mouse model that lacks a functional *Slc25a32* gene to investigate its role in NTC during early embryogenesis. The disruption of the *Slc25a32* gene is embryolethal, and induces morphological abnormalities of NTC in the entire head region of developing mouse embryos, which express completely penetrant NTDs. The majority of *Slc25a32* knockout-induced NTDs were prevented by formate supplementation, but not by 5-mTHF supplementation. Resequencing the *SLC25A32* coding region in human NTD cohorts identified biallelic loss-of-function variants.

Results

Depletion of *Slc25a32* Causes a Failure of Neural Tube Closure in Mice. *Slc25a32* knockout mice (*Slc25a32*$^{gt/gt}$) were generated from the OmniBank ES cell clone IST11480G10, which contained the β-*geo* reporter locus inserted between *Slc25a32* exons 1 and 2 by gene trap technology (15), resulting in a loss-of-function mutation (Fig. 1*A*). The genotype of the mice (Fig. 1*B*) was determined using PCR (Fig. 1*A*) and revealed successful germ-line transmission of the transgenic allele. Reverse transcription PCR (RT-PCR) confirmed the absence of *Slc25a32* mRNA in the mutant embryos (Fig. 1*C*). SLC25A32 protein was undetectable in isolated mitochondria of the *Slc25a32*$^{gt/gt}$ embryos by immunoblot analysis (Fig. 1*D*). These data indicate that the homozygous gene trap insertion successfully disrupted Slc25a32 at both the RNA and protein levels. β-*galactosidase* (*LacZ*) reporter staining indicated that the *Slc25a32* gene is more highly expressed in the cranial region than in the posterior region of embryonic day (E)9.5 embryos, which is the midpoint of murine NTC (Fig. 1*E*).

Initial heterozygote crosses of the *Slc25a32*$^{+/gt}$ mice failed to produce any viable *Slc25a32*$^{gt/gt}$ pups, indicating that homozygous loss of functional *Slc25a32* alleles is incompatible with embryonic development. Timed matings were established to determine when the *Slc25a32*$^{gt/gt}$ embryos die in utero. The heterozygous dams were euthanized at selected time points between E9.5 and E12.5, at which time the uterine contents were analyzed. As seen in Table 1, all *Slc25a32*$^{gt/gt}$ embryos failed to complete NTC. In total, 271 embryos and 31 resorptions from 35 litters were examined between E10 and E12.5. The yolk sacs of all conceptuses were used for PCR genotyping, which indicated that there were 76 *Slc25a32*$^{+/+}$, 135 *Slc25a32*$^{+/gt}$, and 60 *Slc25a32*$^{gt/gt}$ embryos (Table 1).

The majority of the *Slc25a32*$^{gt/gt}$ embryos at E10.5 with NTDs were exencephalic (Fig. 2*A*). A subset of mutant embryos had open neural tubes extending the length from the forebrain to the hindbrain, as well as craniofacial defects (Fig. 2 *B* and *C*). Some *Slc25a32*$^{gt/gt}$ embryos displayed craniorachischisis at E12.5, with an open neural tube extending from the forebrain to the cervical boundary (Fig. 2*D*). At E12.5, the NTD-affected *Slc25a32*$^{gt/gt}$ embryos primarily exhibited exencephaly (Fig. 2 *E* and *F*). All *Slc25a32*$^{gt/gt}$ embryos had open rostral NTDs at either E10.5 or E12.5. Among the 60 *Slc25a32*$^{gt/gt}$ embryos evaluated between E10 and E12.5, 18 embryos had NTC defects from the forebrain to the midbrain, 7 embryos displayed open midbrain NTDs, 26 embryos examined had an open neural tube extending from the midbrain to the hindbrain, and 9 embryos presented with craniorachischisis. Hematoxylin/eosin (HE)-stained histological sections confirmed that E11.5 *Slc25a32*$^{gt/gt}$ embryos exhibited unfused neural folds at the level of the forebrain and the midbrain

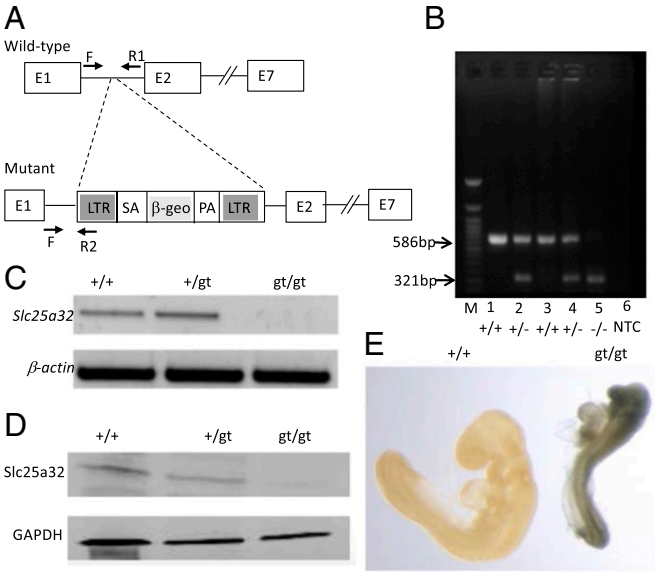

Fig. 1. Characterization of the *Slc25a32* gene knockout in the mouse. (*A*) Genomic structure of *Slc25a32* gene and gene trapping vector design. This schema illustrates the genomic structure of the *Slc25a32* gene. Gene trap insertion of a β-*geo* cassette in the *Slc25a32* locus between exons 1 and 2. The *Slc25a32* gene is disrupted by inserting the β-*geo* (*LacZ*) that encodes β-galactosidase. The arrows indicate location of genotyping forward (F) and reverse (R) primers, wild-type ($^{+/+}$) and mutant (gt/gt) alleles, respectively. LTR, viral long terminal repeat; pA, polyA; SA, splice acceptor. (*B*) Genotyping assays. The extracted genomic DNA is used for PCR genotyping. The banding pattern of the PCR products demonstrates the absence of a 266-bp band in the nullizygous embryos. (*C*) RT-PCR for mRNA. *Slc25a32* mRNA expression was determined in E10 embryos of each possible genotype. RT-PCR analysis was performed with *Slc25a32* or β-*actin* primer as a positive control for cDNA synthesis. (*D*) Immunoblot assay for protein. SLC25A32 protein was detected from isolated mitochondria from E11.5 embryos of each potential genotype. The immunoblot assay was performed with anti-SLC25A32 antibody and anti-GAPDH (glyceraldehyde-3-phosphate dehydrogenase) antibody as a loading control. (*E*) *Slc25a32* gene expression of β-galactosidase (*LacZ*) staining at E9.5. Whole-mount *LacZ* staining of nullizygous and wild-type embryos at E9.5. β-galactosidase was ubiquitously expressed in the *Slc25a32*$^{gt/gt}$ relative to the *Slc25a32*$^{+/+}$ embryos.

(Fig. 2 *G* and *I*), which was not observed in any *Slc25a32*$^{+/+}$ or *Slc25a32*$^{+/gt}$ embryos (Fig. 2*H*).

RNA-Seq Profiling of *Slc25a32* Knockout Embryos at E9. To examine potentially altered gene expression underlying the abnormal phenotypes, RNA-Sequence (Seq) studies were performed on three wild-type (*Slc25a32*$^{+/+}$) and three nullizygous (*Slc25a32*$^{gt/gt}$) E9.0 NTC stage embryos (Fig. 3*A*). Differential expression analysis identified 1,092 genes that were up-regulated, while 630 genes were down-regulated (*SI Appendix*, Fig. S1). Expression level of *Slc25a32* was confirmed to be significantly decreased in the *Slc25a32*$^{gt/gt}$ embryos compared with the *Slc25a32*$^{+/+}$ embryos (Fig. 3*B*). Gene ontology (GO) analysis revealed enrichment for genes ($P < 0.05$) involved in blood circulation, muscle tissue development, cellular ion homeostasis, regulation of cell morphogenesis, and cell fate commitment. The cellular component of GO categories was enriched including: lytic vacuole, lysosome, cell-cell junction, apical part of cell, and extracellular matrix. Among the GO enrichment in molecular function categories, the list included the following: transcriptional activator activity, RNA polymerase II transcription regulatory region sequence-specific binding, core promoter proximal region DNA binding, actin binding, protein heterodimerization activity, and active transmembrane transporter activity (Fig. 3*C*). As shown in *SI Appendix*, Table S1, the list included multiple dysregulated 1C metabolism enzymatic

DEVELOPMENTAL BIOLOGY

Table 1. NTD prevalence in unsupplemented *Slc25a32*$^{gt/gt}$ embryos at E10.5–E12.5

	Embryonic genotype				
Observations	*Slc25a32*$^{+/+}$	*Slc25a32*$^{+/gt}$	*Slc25a32*$^{gt/gt}$	Litters	Resorptions
No. of embryos	76	135	60	35	31
No. of NTDs	0	0	60 (100%)	—	—
p-HWE		1.00		—	—

p-HWE, *P* value of Hardy–Weinberg Equilibrium.

genes. The up-regulated genes include *Fpgs* (Folylpolyglutamyl synthetase) and *Mthfs* (5,10-Methenyltetrahydrofolate synthetase), while down-regulated genes of interest include *Dhfr* (Dihydrofolate reductase) and *Mthfd2l* (Methylenetetrahydrofolate dehydrogenase2-like), both of which are important enzymes involved in folate-mediated 1C metabolism (*SI Appendix*, Table S1). Among the genes whose transcription was significantly (false discovery rate < 0.05) altered in *Slc25a32*$^{gt/gt}$, 22 of them are mouse NTD genes (16) (*SI Appendix*, Table S2). Three mouse NTD genes [*Cdx2* (17), *Lama5*, and *Lrp2* (16)] were up-regulated more than twofold, while the mouse NTD genes (*Pax3* and *Zic3*; ref. 16) were down-regulated more than twofold (*SI Appendix*, Table S2). These represent compelling candidate genes for future interrogation. Ingenuity canonical pathway analysis indicated several up-regulated and down-regulated pathways related to the regulation of genes involved in NTC, including up-regulation of the PCP pathway (18) and down-regulation of Rho family GTPase and RhoA signaling (19) (*SI Appendix*, Fig. S2).

Effect of Maternal Calcium Formate Supplementation in *Slc25a32*-Deficient Mouse. The mitochondrial folate-mediated 1C pathway produces formate to support purine and thymidylate biosynthesis (4, 20). SLC25a32 recognizes and transports THF (13). Disruption of the *Slc25a32* gene affects the transport of THF into the mitochondria, and we demonstrated that providing *Slc25a32*$^{+/gt}$ dams with supplemental formate rescues the developing *Slc25a32*$^{gt/gt}$ embryos from failed NTC. The *Slc25a32*$^{+/gt}$ dams received 0.1 M (a calculated dose of 2,500 mg·kg^{-1}·d^{-1}) calcium formate in their drinking water from the time the pregnancy was recognized (E0.5) throughout gestation. Maternal supplementation with calcium formate in the *Slc25a32*$^{+/gt}$ intercrossed mice failed to generate any viable *Slc25a32*$^{gt/gt}$ pups, consistent with previous experiments with unsupplemented *Slc25a32*$^{+/gt}$ dams. Harvesting litters at selected time points during development, we determined that the *Slc25a32*$^{gt/gt}$ embryos receiving the calcium formate supplementation extended their development, remaining viable until E15.5. In total, we examined 185 embryos and fetuses between E10 and E15.5 from 23 litters. Genotyping revealed that there were 44 *Slc25a32*$^{+/+}$, 95 *Slc25a32*$^{+/gt}$, 32 *Slc25a32*$^{gt/gt}$ embryos, and 14 resorptions (Table 2). In utero calcium formate supplementation resulted in 25 (78.1%) *Slc25a32*$^{gt/gt}$ embryos completing NTC, yet no fetuses survived beyond E15.5 (Fig. 4), while 7 (21.9%) *Slc25a32*$^{gt/gt}$ fetuses had open NTDs (Table 2). This data suggests that 0.1 M calcium formate partially rescues the NTDs by facilitating NTC, yet could not extend normal fetal development to term. We also tried maternal 5-mTHF supplementation throughout the pregnancy. Both 25 and 50 mg/kg doses of 5-mTHF administered by daily oral gavage failed to prevent NTDs (*SI Appendix*, Table S3). Of the six litters, none of the identified 11 *Slc25a32*$^{gt/gt}$ embryos managed to complete NTC.

SLC25A32 Biallelic Loss-of-Function Variants Detected in an NTD Case. Informed by the *Slc25a32*$^{gt/gt}$ NTD phenotype in the mouse, we sought to determine whether *SLC25A32* loss-of-function variants could be found in human NTD subjects. We performed resequencing on 1,009 NTD genomic DNA samples collected from cohorts in both the United States and China (*SI Appendix*, Table S4). Primers used in resequencing are presented in *SI Appendix*, Table S5. Among these samples, we identified two heterozygous loss-of-function (LoF) mutations, c.268_269insAT (p.Trp90fs) and c.391G > T(p.Gly131Ter) in an individual anencephalic fetus (Fig. 4*A*). Allelic segregation demonstrated that the two mutated alleles were located on different chromosomes. The parents' samples were not available for transmission testing. Four rare (MAF < 0.01) heterozygous missense variants (c.382G > A:p.A128T, c.211A > G:p.T71A, c.779G > A:p.S260N, c.164G > T:p.G55V) were detected in four different NTD patients as singletons, three of which were predicted to be disease-causing by MutationTaster (*SI Appendix*, Table S6).

In a previous study (21), the *SLC25A32* nonsense mutation c.425G > A(p.Trp142Ter) was not identified at the cDNA level, suggesting that *SLC25A32* nonsense mutations could be degraded by the nonsense-mediated mRNA decay machinery. It was highly likely that there was no functional SLC25A32 protein produced in our NTD case due to the nonsense-mediated mRNA

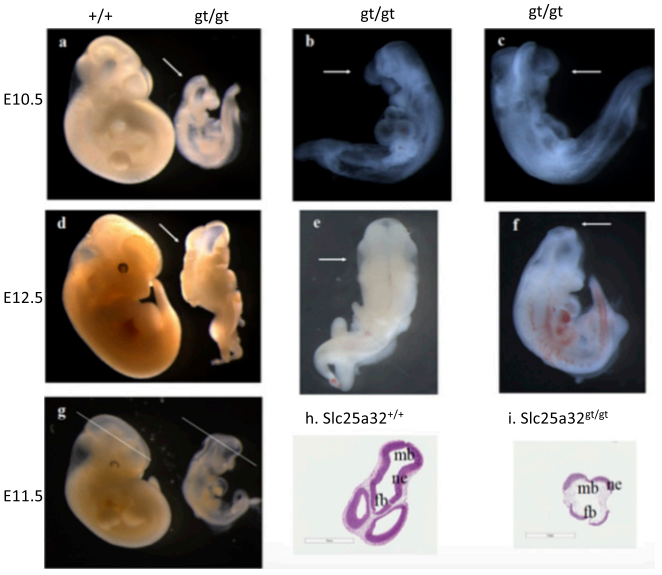

Fig. 2. NTDs in nonsupplemented *Slc25a32*$^{gt/gt}$ embryos (E10.5 and E12.5) and their histological analysis. (*A*) The *Slc25a32*$^{gt/gt}$ embryos display open neural tubes from the forebrain to the midbrain at E10.5. Arrows indicate unfused neural folds in the cranial portion of the *Slc25a32*$^{gt/gt}$ fetuses. (*B* and *C*) Arrow indicate that the nullizygous (*Slc25a32*$^{gt/gt}$) fetuses had exencephaly and craniofacial defects at E10.5. (*D*) At E12.5, the *Slc25a32*$^{gt/gt}$ fetuses present with an open neural tube from the forebrain to the hindbrain. (*E* and *F*) Arrow indicate that the nullizygous (*Slc25a32*$^{gt/gt}$) fetuses exhibited craniorachischisis (E) and exencephaly (F) at E12.5. (*G*) The location of the histological sections of the *Slc25a32* embryos at E11.5 is at the level of the forebrain and the midbrain. (*H*) Arrows indicate the *Slc25a32*$^{+/+}$ fetus with fused neural folds at the level of the forebrain and the midbrain. (*I*) Arrows indicate the *Slc25a32*$^{gt/gt}$ embryo with unfused neural folds, precursors to exencephaly and craniofacial defects. (Scale bars: 1 mm.) fb, forebrain; mb, midbrain; ne, neuroepithelium.

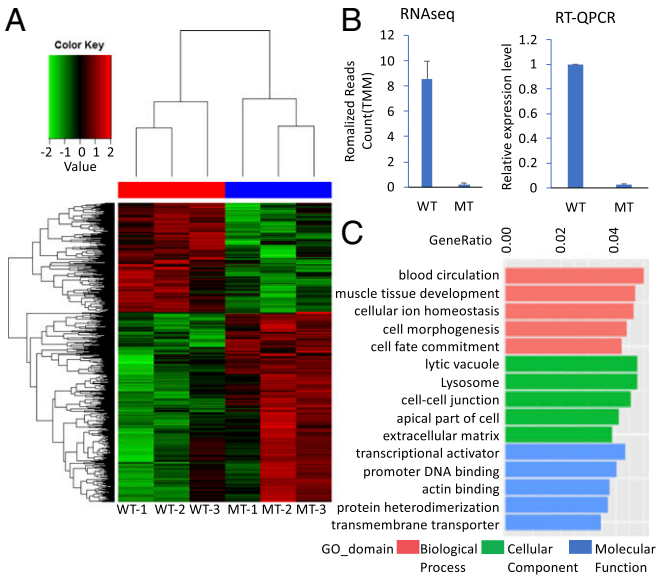

Fig. 3. RNA-Seq analysis of inactivation *Slc25a32* gene in E9.0 embryos. (*A*) Heat map of RNA-Seq data indicates the DEGs patterns between *Slc25a32*$^{+/+}$ (n = 3) and *Slc25a32*$^{gt/gt}$ (n = 3) E9.0 embryos. (*B*) RNA-Seq data shows the expression level of *Slc25a32* by normalized reads counts (TMM) in the *Slc25a32*$^{gt/gt}$ embryos compared with the *Slc25a32*$^{+/+}$ embryos at E9.0. The quantitative real-time PCR (qRT-PCR) data showed the similar result with RNA-Seq data. The qRT-PCR analysis was performed with *Slc25a32* primer, and β-*actin* primer was used as a housekeeping gene. (*C*) RNA-Seq data reveals GO enrichment with the top five classifications including biological process, cellular component, and molecular function in the *Slc25a32*$^{gt/gt}$ embryos compared with the *Slc25a32*$^{+/+}$ embryos at E9.0. The bar graph represents dysregulated genes in each ontological classification (P < 0.05).

decay machinery. Considering the possibility that even a small amount of mRNA might be translated into SLC25A32 protein before its degradation, we tested the function of the two LoF variants using subcellular localization and the *glyB* complementation assay (12, 13). Subcellular localization demonstrated that the two mutations did not abolish SLC25A32 colocalization within the mitochondria (Fig. 4*B*). In the *glyB* complementation assay, neither of the mutant proteins were able to rescue the *glyB* auxotrophic phenotype (Fig. 4*C*). Previous work demonstrated that Trp142 is necessary to form a pi–cation interaction, which is necessary for THF uptake and transport (13). The two mutations identified here were predicted to disrupt the Trp142 residue, which might abolish the ability of SLC25A32 to bind THF.

Discussion

Low folate status has been known to increase the risk for an NTD-affected pregnancy. Studies conducted over the past 30 y have consistently shown that maternal periconceptional supplementation with FA can reduce the prevalence of NTDs by more than 80% (5, 6). Extensive efforts have been made trying to learn how supplemental FA benefits developing embryos by modifying variants within the folate 1C metabolic pathway, as well as to develop new strategies to prevent FA-resistant NTDs. Inactivation of the cytosolic folate 1C enzymes, methylenetetrahydrofolate reductase (*Mthfr*) and methylenetetrahydrofolate dehydrogenase 1 (*Mthfd1*), do not cause NTDs in the mouse (22, 23); however, variants in these genes have been associated with increased NTD risk in human studies (24–27). The one known exception is the serine hydroxymethyltransferase 1 (*Shmt1*) null mice, which express NTDs but only under folate-deficient dietary conditions (28). By contrast, in transgenic mouse models lacking functional aminomethyltransferase (*Amt*) and *Mthfd1l* genes that encode enzymes involved in mitochondrial folate 1C metabolism, NTDs are frequent developmental outcomes without requiring any folate-deficient dietary conditions to express the abnormal phenotype (29, 30). In the present study, embryos lacking a functional *Slc25a32* gene, which encodes mitochondrial folate transporter, invariably had an NTD, either exencephaly or craniorachischisis, consistent with the NTD phenotypes observed in other mouse models that impact mitochondrial 1C metabolism.

Formate is a non-THF–linked intermediate in 1C metabolism. Metabolic sources of formate are classified as either folate-independent or folate-dependent (20). Mitochondrial 1C metabolism plays a key role in formate production, which is transported from the mitochondria to the cytoplasm for de novo purine and pyrimidine synthesis. Disruption of mitochondrial 1C metabolism can reduce formate yield and impair nucleotide synthesis, cell proliferation, and NTC morphogenesis (31). In our study, we observed that maternal calcium formate supplementation of the *Slc25a32*$^{+/gt}$ dams partially rescues the *Slc25a32*$^{gt/gt}$ embryos from NTDs, whereas the 5-mTHF supplementation failed to prevent NTDs in the mutant embryos. This was similar to the rescue provided by maternal formate supplementation to *Mthfd1l*$^{z/+}$ (30) and *Gldc*$^{gt/+}$ dams (32). The failure of formate to rescue the NTDs completely might be related to the fact that *Slc25a32*$^{gt/gt}$ mice are also auxotrophic for glycine, making the demand for additional 1C units more dire and perhaps requiring higher concentrations of formate than were utilized in this study. Future supplementation studies on *Slc25a32*$^{gt/gt}$ mice with both formate and glycine administration are warranted.

A review of the current literature indicates that there are three studies reporting *SLC25A32* variants associated with human diseases: Two of them described *SLC25A32* functional variants associated with riboflavin-responsive exercise intolerance (21, 33), which was attributed to SLC25A32's flavin adenine dinucleotide (FAD) transporter function (34), while the other study reported a SNP (rs2241777) at the 3′ UTR of *SLC25A32* associated with plasma folate levels and bone fractures in postmenopausal Japanese women (35). The *SLC25A32* gene was also reported to be overexpressed in ovarian and breast cancer patients in a large human cancer cohort (36). In the present study, informed by the *Slc25a32*$^{gt/gt}$ mouse NTD phenotype, we identified *SLC25A32* biallelic LoF variants in a human cranial NTD patient.

Table 2. The impact of maternal calcium formate supplementation on NTC in *Slc25a32*$^{gt/gt}$ embryos at E10–15.5

	Embryonic genotype				
Observations	*Slc25a32*$^{+/+}$	*Slc25a32*$^{+/gt}$	*Slc25a32*$^{gt/gt}$	Litters	Resorptions
No. of embryos	44	95	32	23	14
No. of NTD	0	0	7 (21.9%)	—	—
No. of NTC	44	95	25 (78.1%)	—	—
p-HWE		0.13		—	—

p-HWE, P value of Hardy–Weinberg Equilibrium.

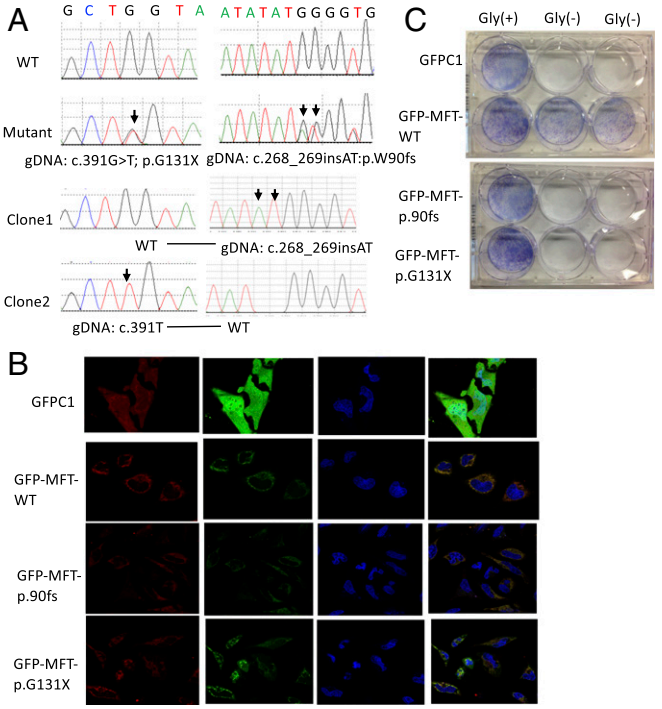

Fig. 4. Biallelic loss-of-function mutations identified in an NTD case. (*A*) Sanger sequencing chromatogram. Clone1 and Clone2 were PCR clone sequencing. It indicated that the two mutations were in two haplotypes/chromosomes. (*B*) Subcellular localization of wild-type *SLC25A32* and two mutant *SLC25A32*. The mitochondria (red) were stained using MitoSOX Red Mitochondrial Superoxide Indicator. Green indicated GFP-tagged SLC25A32 or GFP protein. Wild-type and mutant SLC25A32 localized to mitochondria. (*C*) glyB complementation of glycine auxotrophy with SLC25A32 wild-type and mutant proteins. The blue color indicated Giemsa-stained cells. Wild-type SLC25A32 plasmid could rescue GlyB auxotophy but not mutant SLC25A32 plasmids.

Our study did not show mitochondrial metabolic profiles, including THF levels in *Slc25a32*$^{gt/gt}$ embryos, which was one of the limitations of this study. However, formate supplementation partially rescued NTD phenotypes in *Slc25a32*$^{gt/gt}$ embryos, indirectly suggesting the presence of a THF deficiency in the mitochondria. In future studies, the 1C metabolomic profiles of the *Slc25a32* mutant mouse will provide novel insight for alternative therapeutic strategies for prevention of folate resistant NTDs. Although, tetrahydrofolate is the folate form expected to be transported by MFT, there is yet no direct evidence for the specificity of that process, thus the *Slc25a32* mutant mouse model will also be useful for providing novel insight into the specificity of the transport function of the Slc25a32 protein.

Materials and Methods

Generation of *Slc25a32* Mice. A transgenic mouse model of the gene *Slc25a32* was generated by microinjection of OmniBank ES cell clones (IST11480G10; encoding the gene *Slc25a32*) obtained from the Texas A&M Institute for Genomic Medicine. The gene trap mutations were produced by using the insertion of gene trap vector, β-geo (*LacZ*) reporter (encoded by β-galactosidase), into ES cells derived from the C57BL/6 strain. All experimental mice were housed in accordance with guidelines approved by the Institutional Animal Care and Use Committee of The University of Texas at Austin. All mice were fed a PicoLab diet no. 20 (3 ppm of folic acid) and water, ad libitum, and were maintained on a 12-h light/dark cycle in a temperature-controlled room.

Mice Genotyping Assay. Genomic DNA was extracted from the yolk sacs of embryos or the tail of young pups for genotyping assays. The samples were prepared by DirectPCR Lysis Reagent and Proteinase K (Viagen Biotech). The PCR genotyping was performed using one primer pair (Slc25a32F: 5′-agtgtgtgagccggtgcttt -3′ and Slc25a32R: 5′- tgggtcctgtggaaaggcta -3′) to detect the wild-type allele (586 bp) and the other primer pair (Slc25a32F: 5′-agtgtgtgagccggtgcttt -3′ and V76R: 5′- CCAATAAACCCTCTTGCAGTTGC -3′) to detect the mutant allele (321 bp). QIAGEN Multiplex PCR Master Mix (catalog no. 206145; QIAGEN) was used for PCR following the product handbook.

β-Galactosidase (*LacZ*) Staining and Histology Analysis. For detecting reporter gene expression, β-galactosidase staining of E9.5 embryos were carried out using 5-bromo-4-chloro-3-indolyl β-D-galactoside (X-Gal) stock (Sigma), marking a nuclear localized *lacZ* transgene. For histological analyses, the E11.5 fetuses were fixed in 10% neutral buffered formalin and embedded in paraffin. They were sectioned at 4-μm thickness and stained with HE.

RT-PCR and qRT-PCR. For RT-PCR analysis, total mRNA was extracted from whole mouse embryos of all *Slc25a32* potential genotypes at E10 using TRIzol Reagent (Invitrogen). First-strand cDNA was synthesized by cDNA Reverse Transcription Kit (Applied Biosystems). PCR was carried out with designed primer pairs of the *Slc25a32* gene forward (5′-GGAGCCATGAC-TCTGTGCAT-3′) and reverse (5′-TCCACCGATGCCTTCTTTCC-3′) to amplify a 441-bp amplicon, and β-*actin* primer as a positive control forward (5′-CCACCATGTACCCAGGCATT-3′) and reverse (5′-AGGGTGTAAAACGCAGC-TCA-3′) (253 bp). For qRT-PCR analysis, the total mRNA was prepared from whole E9.5 embryos of all genotypes, and cDNA was synthesized as described above. The mRNA levels were quantitatively measured by using SsoAdvanced Universal SYBR Green Supermix (Bio-Rad). The *Slc25a32* and β-*actin* primers were used as a control, as described above.

Immunoblot Analysis. To detect the *Slc25a32* protein, mitochondria were isolated from whole E11.5 fetuses of all three genotypes using the Mitochondria Isolation Kit (Thermo Fisher Scientific). The samples were sonicated in RIPA lysis buffer [50 mM Tris·HCl pH 8.0, 150 mM NaCl, 0.1% Triton X-100, 0.5% sodium deoxycholate, 0.1% SDS, 0.1 mM sodium orthovanadate, 1 mM NaF, and Protease inhibitors tablet (Roche)]. A Bradford assay was performed to determine the protein concentrations (Bio-Rad). The protein was immunoblotted with rabbit polyclonal anti-SLC25A32 (Thermo Fisher Scientific) at a concentration of 1:1,000, GAPDH (Cell Signaling) as a control at a dilution of 1:5,000, and 1RDye 800CW Goat anti-Rabbit IgG (LI-COR) at a concentration of 1:10,000 to probe the antibodies against the target protein.

RNA-Seq Analysis. Total mRNA was isolated from three E9.0 whole *Slc25a32*$^{+/+}$ and *Slc25a32*$^{gt/gt}$ embryos using TRIzol Reagent (Invitrogen), as described above. The concentration of the RNA was determined using a Nanodrop ND-1000 Spectrophotometer (NanoDrop Technologies). The integrity of RNA was evaluated using a 1% denaturing RNA gel and an Agilent Technologies 2100 Bioanalyzer. Sequencing of the cDNA libraries was performed on an Illumina Hiseq 4000 (Quick Biology). Differentially expressed genes (DEGs) were determined by fold change >1.5 (logFC > 0.58) and a $P < 0.05$, genes with <1 count per million (cpm). All obtained datasets were analyzed for GO, Kyto Encyclopedia of Genes and Genomes, and reactome analysis with enriched terms, and for Ingenuity Pathway Analysis including the canonical pathway.

Calcium Formate Supplementation. *Slc25a32*$^{+/gt}$ dams were randomly assigned to a control or to a calcium formate supplementation group. The supplementation was administered daily, immediately after detection of the vaginal plug (0.5 dpc). Pregnant dams were given 0.1 M (2,500 mg) calcium formate·kg^{-1}·d^{-1} directly in the drinking water based on an average daily water intake of 5 mL/d for a 25-g mouse (30) and were continued throughout pregnancy.

5-mTHF Supplementation. *Slc25a32*$^{+/gt}$ dams were randomly assigned to a 25 or 50 mg/kg 5-mTHF supplementation group. The supplement was administered daily, via oral gavage, starting on the day the vaginal plug (0.5 dpc) was detected. Pregnant dams were administered a water solution of 5-mTHF in a volume of 10 mL·kg^{-1}·d^{-1} until the dams were euthanized on 12.5 dpc.

***SLC25A32* DNA Resequencing.** We resequenced 1,009 NTD genomic DNA samples collected from US and Chinese cohorts (*SI Appendix*, Table S3), with the approval from the respective institutional review boards of The University of Texas at Austin, Peking University, Capital Institute of Pediatrics, and China Medical University. US NTD samples were collected from Dell Children's Medical Center between 2010 and 2017, which was post-FA fortification. Chinese NTDs from Peking University were collected from 2000 to 2014 in a population-based birth defect surveillance program, which has been previously described elsewhere (37). Chinese NTD patients recruited

from the Capital Institute of Pediatrics were described in recently published papers (38, 39). Samples provided by China Medical University were collected in Shengjing Hospital without supplemental FA documentation. We obtained written informed consent from the participants' parents. Details on the DNA sequencing procedures, haplotype analysis, and primers are included in *SI Appendix, Supplementary Methods*.

Subcellular Localization. *SLC25A32* wild-type plasmid was obtained from Genscript (Clone ID: OHu10082C) and subcloned into pcDNA3.1+C-eGFP. SLC25A32 mutant plasmids containing c.268_269insAT(p.Trp90fs) and c.391G > T(p.Gly131Ter) were made by GeneArt Site-Directed Mutagenesis System (catalog no. A13282; Thermo Fisher Scientific) following the protocol in the user's manual. HeLa cell line was used for *SLC25A32* subcellular localization studies. One day before transfection, cells were seeded in 35-mm glass bottom dishes (In Vitro Scientific) at 10,000 cells per dish. Lipofectamine 2000 Transfection Reagent (catalog no. 11668019; Thermo Fisher Scientific) was used for eGFP-tagged *SLC25A32* wild-type and mutant vectors (500 ng per dish) transfection. Forty-eight hours later, cells were stained with MitoSOX Red (catalog no. M36008; Thermo Fisher Scientific) for mitochondrial and Hoechst 3342 (catalog no. 66249; Thermo Fisher Scientific) for nuclei. Cells were examined and photographed by a laser scanning confocal microscope (LSM710; Leica).

GlyB Complementation. GlyB and CHO-K1 cells were cultured in MEM-alpha medium (catalog no. 12561056; Thermo Fisher Scientific) with 10% FBS. GlyB complementation assay was followed from Moran and coworkers' publication in 2004 (12) and 2011 (13).

Statistical Analysis. Genotyping frequencies were compared by Hardy–Weinberg equilibrium and analyzed using a χ^2 test. The data were analyzed by mean ± SE with Student's *t* test, and any *P*s < 0.05 were considered statistically significant.

ACKNOWLEDGMENTS. We thank the families for their participation in this study, Dr. Richard G. Moran (Virginia Commonwealth University, Richmond, VA) for providing GlyB and CHO-K1 cells, and Dr. Yue Li for her excellent assistance with the confocal microscopy. This project was supported by NIH Grants HD081216, HD083809, and HD067244 (to R.H.F.); Chinese Academy of Medical Sciences Initiative for Innovative Medicine Grant 2016-I2M-1-008 (to T.Z.); 973 Program of China Grant 2013CB945400 (to T.Z. and Z.Y.); National Key Research and Development Program, Ministry of Science and Technology, P.R. China Grant 2016YFC1000501 (to A.R.); and National Natural Science Foundation of China Grant 81472987 (to L.W.).

1. Zaganjor I, et al. (2016) Describing the prevalence of neural tube defects worldwide: A systematic literature review. *PLoS One* 11:e0151586.
2. Nikolopoulou E, Galea GL, Rolo A, Greene ND, Copp AJ (2017) Neural tube closure: Cellular, molecular and biomechanical mechanisms. *Development* 144:552–566.
3. Copp AJ, Greene ND (2013) Neural tube defects–Disorders of neurulation and related embryonic processes. *Wiley Interdiscip Rev Dev Biol* 2:213–227.
4. Tibbetts AS, Appling DR (2010) Compartmentalization of Mammalian folate-mediated one-carbon metabolism. *Annu Rev Nutr* 30:57–81.
5. Berry RJ, et al.; Collaborative Project for Neural Tube Defect Prevention (1999) Prevention of neural-tube defects with folic acid in China. China-U.S. *N Engl J Med* 341: 1485–1490, and erratum (1999) 341:1864.
6. Anonymous; MRC Vitamin Study Research Group (1991) Prevention of neural tube defects: Results of the Medical Research Council Vitamin Study. *Lancet* 338:131–137.
7. Copp AJ, Stanier P, Greene NDE (2013) Neural tube defects: Recent advances, unsolved questions, and controversies. *Lancet Neurol* 12:799–810.
8. Lane AN, Fan TW (2015) Regulation of mammalian nucleotide metabolism and biosynthesis. *Nucleic Acids Res* 43:2466–2485.
9. Crider KS, Yang TP, Berry RJ, Bailey LB (2012) Folate and DNA methylation: A review of molecular mechanisms and the evidence for folate's role. *Adv Nutr* 3:21–38.
10. Pike ST, Rajendra R, Artzt K, Appling DR (2010) Mitochondrial C1-tetrahydrofolate synthase (MTHFD1L) supports the flow of mitochondrial one-carbon units into the methyl cycle in embryos. *J Biol Chem* 285:4612–4620.
11. Titus SA, Moran RG (2000) Retrovirally mediated complementation of the glyB phenotype. Cloning of a human gene encoding the carrier for entry of folates into mitochondria. *J Biol Chem* 275:36811–36817.
12. McCarthy EA, Titus SA, Taylor SM, Jackson-Cook C, Moran RG (2004) A mutation inactivating the mitochondrial inner membrane folate transporter creates a glycine requirement for survival of Chinese hamster cells. *J Biol Chem* 279:33829–33836.
13. Lawrence SA, Hackett JC, Moran RG (2011) Tetrahydrofolate recognition by the mitochondrial folate transporter. *J Biol Chem* 286:31480–31489.
14. Ducker GS, Rabinowitz JD (2017) One-carbon metabolism in health and disease. *Cell Metab* 25:27–42.
15. Zambrowicz BP, et al. (2003) Wnk1 kinase deficiency lowers blood pressure in mice: A gene-trap screen to identify potential targets for therapeutic intervention. *Proc Natl Acad Sci USA* 100:14109–14114.
16. Wilde JJ, Petersen JR, Niswander L (2014) Genetic, epigenetic, and environmental contributions to neural tube closure. *Annu Rev Genet* 48:583–611.
17. Savory JG, Mansfield M, Rijli FM, Lohnes D (2011) Cdx mediates neural tube closure through transcriptional regulation of the planar cell polarity gene Ptk7. *Development* 138:1361–1370.
18. Nishimura T, Honda H, Takeichi M (2012) Planar cell polarity links axes of spatial dynamics in neural-tube closure. *Cell* 149:1084–1097.
19. Kinoshita N, Sasai N, Misaki K, Yonemura S (2008) Apical accumulation of Rho in the neural plate is important for neural plate cell shape change and neural tube formation. *Mol Biol Cell* 19:2289–2299.
20. Brosnan ME, Brosnan JT (2016) Formate: The neglected member of one-carbon metabolism. *Annu Rev Nutr* 36:369–388.
21. Schiff M, et al. (2016) SLC25A32 mutations and riboflavin-responsive exercise intolerance. *N Engl J Med* 374:795–797.
22. Li D, et al. (2005) Maternal methylenetetrahydrofolate reductase deficiency and low dietary folate lead to adverse reproductive outcomes and congenital heart defects in mice. *Am J Clin Nutr* 82:188–195.
23. Beaudin AE, Perry CA, Stabler SP, Allen RH, Stover PJ (2012) Maternal Mthfd1 disruption impairs fetal growth but does not cause neural tube defects in mice. *Am J Clin Nutr* 95:882–891.
24. Jiang J, Zhang Y, Wei L, Sun Z, Liu Z (2014) Association between MTHFD1 G1958A polymorphism and neural tube defects susceptibility: A meta-analysis. *PLoS One* 9: e101169.
25. Prasoona KR, et al. (2016) Paternal transmission of MTHFD1 G1958A variant predisposes to neural tube defects in the offspring. *Dev Med Child Neurol* 58:625–631.
26. Yan L, et al. (2012) Association of the maternal MTHFR C677T polymorphism with susceptibility to neural tube defects in offsprings: Evidence from 25 case-control studies. *PLoS One* 7:e41689.
27. Yang Y, Chen J, Wang B, Ding C, Liu H (2015) Association between MTHFR C677T polymorphism and neural tube defect risks: A comprehensive evaluation in three groups of NTD patients, mothers, and fathers. *Birth Defects Res A Clin Mol Teratol* 103:488–500.
28. Beaudin AE, et al. (2011) Shmt1 and de novo thymidylate biosynthesis underlie folate-responsive neural tube defects in mice. *Am J Clin Nutr* 93:789–798.
29. Narisawa A, et al. (2012) Mutations in genes encoding the glycine cleavage system predispose to neural tube defects in mice and humans. *Hum Mol Genet* 21: 1496–1503.
30. Momb J, et al. (2013) Deletion of Mthfd1l causes embryonic lethality and neural tube and craniofacial defects in mice. *Proc Natl Acad Sci USA* 110:549–554.
31. Martiniova L, Field MS, Finkelstein JL, Perry CA, Stover PJ (2015) Maternal dietary uridine causes, and deoxyuridine prevents, neural tube closure defects in a mouse model of folate-responsive neural tube defects. *Am J Clin Nutr* 101:860–869.
32. Pai YJ, et al. (2015) Glycine decarboxylase deficiency causes neural tube defects and features of non-ketotic hyperglycinemia in mice. *Nat Commun* 6:6388.
33. Hellebrekers DMEI, et al. (2017) Novel SLC25A32 mutation in a patient with a severe neuromuscular phenotype. *Eur J Hum Genet* 25:886–888.
34. Spaan AN, et al. (2005) Identification of the human mitochondrial FAD transporter and its potential role in multiple acyl-CoA dehydrogenase deficiency. *Mol Genet Metab* 86:441–447.
35. Urano T, et al. (2014) Polymorphism of SLC25A32, the folate transporter gene, is associated with plasma folate levels and bone fractures in Japanese postmenopausal women. *Geriatr Gerontol Int* 14:942–946.
36. Louhimo R, et al. (2016) Data integration to prioritize drugs using genomics and curated data. *BioData Min* 9:21.
37. Liu J, et al. (2016) Prevalence and trend of neural tube defects in five counties in Shanxi province of Northern China, 2000 to 2014. *Birth Defects Res A Clin Mol Teratol* 106:267–274.
38. Chen S, et al. (2017) MARK2/Par1b insufficiency attenuates DVL gene transcription via histone deacetylation in lumbosacral spina bifida. *Mol Neurobiol* 54:6304–6316.
39. Li H, et al. (2018) Genetic contribution of retinoid-related genes to neural tube defects. *Hum Mutat* 39:550–562.